Eur. Radiol. (2001) 11: 2516–2520
DOI 10.1007/s003300100835

Claudius W. König
Christina Pfannenberg
Jochen Trübenbach
Christopher Remy
Gabriele M. Böhmer
Peter Ruck
Claus D. Claussen

MR cholangiography in the diagnosis of sclerosing cholangitis in Langerhans' cell histiocytosis

Received: 10 July 2000
Revised: 5 January 2001
Accepted: 10 January 2001
Published online: 1 March 2001

C. W. König (✉) · C. Pfannenberg · J. Trübenbach · C. Remy · C. D. Claussen
Department of Diagnostic Radiology, University of Tübingen, Hoppe-Seyler-Strasse 3, 72076 Tübingen, Germany
E-mail: claudius.koenig@t-online.de
Phone: +49-7071-2982087

G. M. Böhmer
Department of Gastroenterology, University of Tübingen, Otfried-Müller-Strasse 10, 72076 Tübingen, Germany

P. Ruck
Institute of Pathology, University of Tübingen, Liebermeisterstrasse 8, 72076 Tübingen, Germany

Present address: G. M. Böhmer, Institute for Clinical Metabolic Research, Technical University of Dresden, Fetscherstrasse 74, 01307 Dresden, Germany

Abstract Langerhans' cell histiocytosis (LCH) is a disorder of histiocytic proliferation that primarily affects infants. Imaging findings of a rare case of lung and liver involvement in an adult are presented. High-resolution computed tomography (HRCT) of the lungs showed confluent thin-walled cystic air spaces compatible with advanced LCH. Liver CT and MRI revealed unspecific signs of fatty infiltration. Irregular widening of peripheral bile ducts was displayed in breath-hold MR cholangiography. This pattern is considered characteristic for sclerosing cholangitis and should support the diagnosis of LCH in case of concomitant cystic pulmonary disease, even in adult patients.

Keywords Langerhans' cell histiocytosis · Sclerosing cholangitis · MR cholangiopancreatography

Introduction

Langerhans' cell histiocytosis (LCH), previously known as histiocytosis X, encompasses clinically heterogeneous but histologically similar disorders including eosinophilic granuloma, Hand-Schüller-Christian lipogranulomatosis and Abt-Letterer-Siwe disease. Systemic disease with a leukemia-like course primarily affects infants and is rarely found in adults [1, 2, 3, 4]. We present the imaging findings of lung and liver involvement in an adult patient with rapidly progressing LCH.

Case report

A 68-year-old female patient presented with fever, night sweat, weight loss, leukocytosis, elevated erythrocyte sedimentation rate (ESR), anemia, and elevated liver enzymes. Diabetes insipidus requiring vasopressin substitution had been diagnosed 3 years previously. A chest plain film showed ill-defined linear opacities in the right upper lobe with cavitated zones, suggesting tuberculosis. A biopsy during thoracoscopy revealed active fibrosing alveolitis with proliferating pneumocytes and focal fibrosis. Microbiological studies were negative; hence, prednisolone was given. An initial endoscopic retrograde cholangiopancreatography (ERCP) and liver sonography were unremarkable except for mild hepatomegaly and gallstones. A bone marrow biopsy demonstrated focal fibrosis and numerous multiclonal plasmocytes.

The liver enzymes further increased over a period of 4 months to a maximum of GOT 97 U/l, GPT 285 U/l, LDH 420 U/l, AP 2050 U/l, gamma-GT 2418 U/l, and bilirubin 4.5 mg/dl. The patient developed mild jaundice and an itching maculopapular rash with ulcerous skin lesions. Laboratory tests ruled out viral or other infection. There was no evidence of concomitant anterior pituitary deficiency, skeletal involvement, systemic amyloidosis, hepatocellular carcinoma, or other malignancies. A mild thrombocytopenia (110,000/μl) developed. The imaging findings are described herein. Percutaneous liver biopsy revealed granulomatous inflammation with histiocytic infiltrates, periportal fibrosis, destructed next to proliferating bile ducts and focal steatosis, compatible with (primary) sclerosing cholangitis (Fig. 1). Lung biopsies were moderately and the liver specimen markedly immunoreactive for S-100 protein, so the diagnosis of Langerhans' cell histiocytosis was established. Ultrastructural analysis was not performed. Despite steroid therapy, the patient died 6 months after onset of pulmonary and hepatic involvement.

In high-resolution computed tomography (HRCT) of the lung circumscribed areas of low attenuation were found bilaterally with predominance in the apex and the upper segment of the lower lobe, resembling localized perilobular emphysematous rarefaction of lung parenchyma (Fig. 2). Confluent thin-walled bullous changes were found rather than small cystic air spaces. There was no evidence of micronodules, pneumothorax, lymphadenopathy, or pleural effusion.

Ultrasonography of the liver showed mild hepatomegaly with an inhomogeneous, partly hyperechoic echotexture and some intrahepatic bile duct dilatation. Liver parenchyma was markedly inhomogeneous on unenhanced CT. Contrast-enhanced CT scans allowed better definition of finger-shaped areas of low attenuation suggesting circumscribed fatty infiltration (Fig. 3). In MRI a focal area of hyperperfusion was depicted on T1-weighted images (Fig. 4b) immediately after administration of Gd-DTPA (Schering, Berlin, Germany). Hypointense infiltration of the liver parenchyma was best shown in the delayed contrast-enhanced T1-weighted series using spectral fat saturation (Fig. 4c), whereas inhomogeneity was only moderate without fat suppression (Fig. 4a, b). Opposed-phase imaging was not performed. T2-weighted images were slightly inhomogeneous due to focal bile duct dilatation.

Endoscopic retrograde cholangiopancreatography (ERCP) was largely unremarkable except for moderate rarefaction of non-dilated intrahepatic bile ducts. Breath-hold MR cholangiopancreatography (MRCP) using the rapid acquisition with relaxation enhancement (RARE) technique [5] revealed peripheral focal cholestasis in each section of the liver (Fig. 5). Multiple slightly dilated bile ducts were displayed showing wall irregularities, filling defects and high-grade obstruction. No extensive ductal dilatation was present. Few segmental branches were displayed with loss of normal tapering. The remaining ducts appeared irregularly defined, partly "ragged," with ductal stenosis and filling defects next to normal non-dilated ducts. The extrahepatic bile ducts appeared unremarkable with the exception of a short signal void in the CBD next to the hepatic ducts' confluence. Breath-hold MRCP was performed on a 1.5-T System (Magnetom Vision, Siemens, Erlangen, Germany) equipped with a phased-array surface coil. Half Fourier acquisition single-shot turbo spin-echo (HASTE) multislice sequences [effective TE 95 ms, echo train length (ETL) 128, echo spacing 11.9 ms, 9 slices, section thickness 4 mm, field of view (FOV) 300 mm, acquisition time 18 s] were applied in coronal and semicoronal (LAO 30°) view. Repeated projection acquisitions

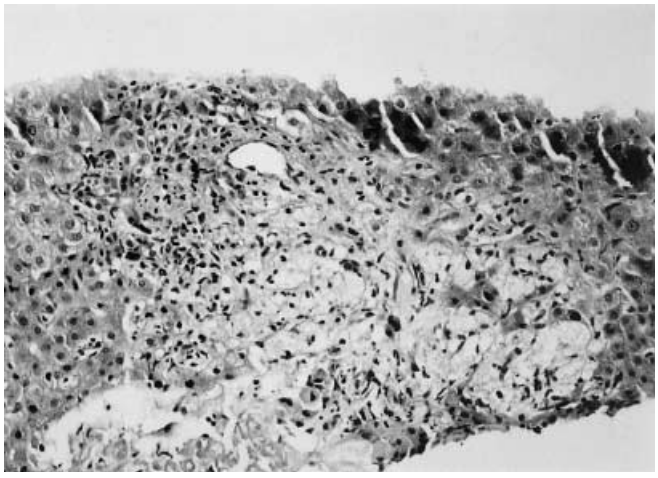

Fig. 1 Liver biopsy reveals fibrosis, chronic inflammatory infiltrates, and the absence of interlobular bile ducts in some portal tracts. Histiocytic infiltrates were highly immunoreactive for S-100 protein

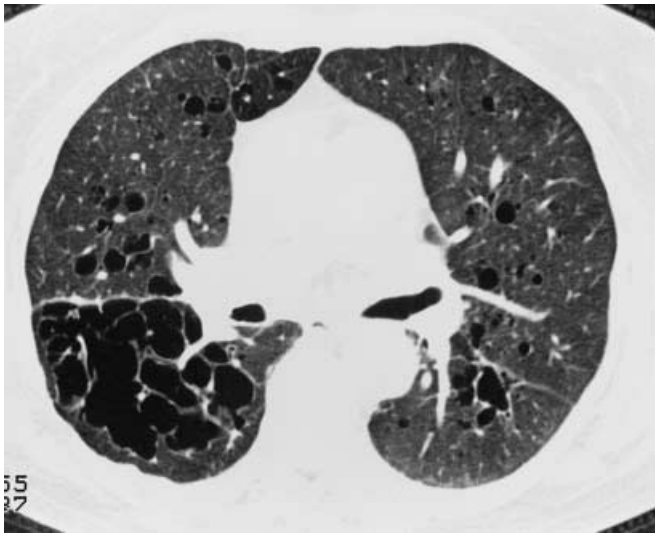

Fig. 2 Lung involvement in Langerhans' cell histiocytosis (LCH). Multiple, partly confluent thin-walled cystic air spaces predominating in the upper zones of the lung is shown on high-resolution CT

Fig. 3 Contrast-enhanced CT with finger-shaped areas of low attenuation suggesting circumscribed fatty infiltration of the liver parenchyma

using the RARE sequence were performed in varying (semi-)coronal views (effective TE 1200 ms, ETL 240, echo spacing 11.5 ms, section thickness 30–80 mm, acquisition time 4 s).

Discussion

Langerhans' cell histiocytosis (LCH) is a disorder of histiocytic proliferation with predominance in young children, characterized by inappropriate infiltration with histiocytes similar to the dendritic antigen-presenting Langerhans' cells of the skin, esophagus, vagin, and buccal mucosa [1, 2, 3, 4]. It is prevalently considered to be a disorder reactive to infection or a sequel of aberrant immune regulation [1], but Willman et al. demonstrated clonality in LCH cells, supporting a neoplastic origin [3]. The biological behavior is highly variable. While patients with solitary bone lesions [6, 7] have a good prognosis, polyostotic disease, signs of systemic involvement, such as thrombocytopenia and hepatosplenomegaly, and age under 2 years at diagnosis are predictors of decreased survival. Diabetes insipidus, skin lesions, and interstitial lung disease are the most common extraskeletal manifestations [1].

In patients with lung involvement Brauner et al. [8] and Moore et al. [9] described patterns of cystic air spaces, reticulation, nodules, and ground-glass opacities with predominance in the upper and middle lung zones. Evidence was found that lesions progress from small nodules to cavitated nodules, thick-walled air spaces, and finally to confluent cysts. Our findings of confluent thin-walled bullous changes without micronodules are

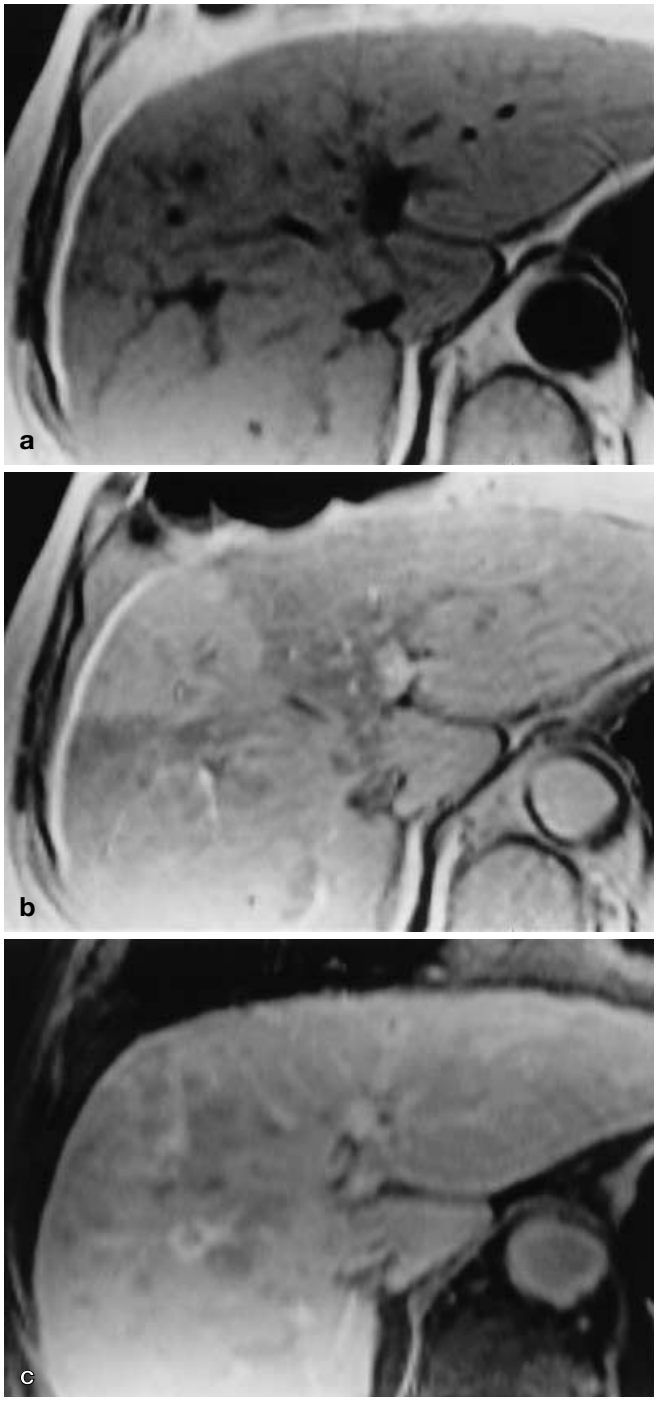

Fig. 4 **a** Unenhanced T1-weighted MR image (fast low-angle shot 126/4.8/75) with poor lesion-to-liver-contrast. **b** Early-phase contrast enhanced T1-weighted image depicts a wedge-shaped area of hyperperfusion. **c** Delayed scan with spectral fat saturation reveals extensive hypointense infiltration of the parenchyma, predominating the periportal areas. A phased-array surface coil was used

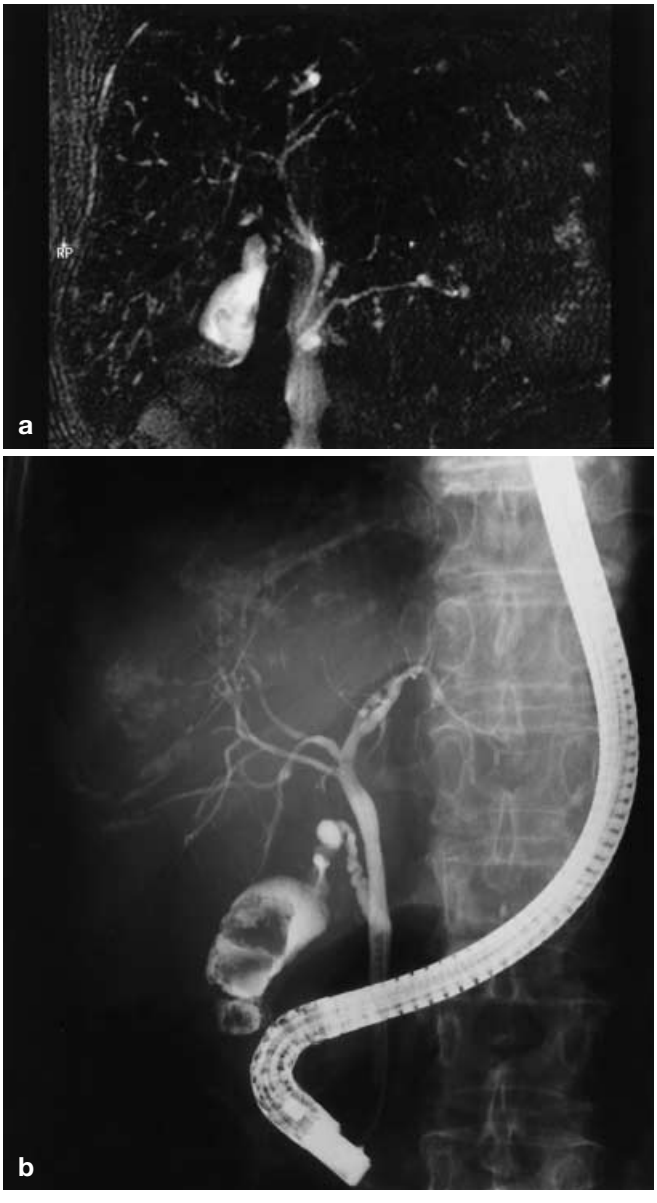

Fig. 5 **a** Rapid acquisition with relaxation enhancement projection acquisition displays multiple moderately dilated bile ducts with irregular definition and ductal obstruction. Note gallbladder stones. See text for details. Cerebrospinal fluid of the lumbar spine is artificially displayed. A short signal void in the common bile duct is considered an artifact caused by the hepatic artery. **b** Corresponding endoscopic retrograde cholangiopancreatography

compatible with LCH in an advanced stage according to Brauner et al. [8]. The thin-walled boundaries clearly differentiate the findings from emphysema, and predominance bilaterally in the upper and middle sections with sparing of the lung bases is typical of LCH.

Liver involvement in disseminated LCH is characterized by histiocytic infiltration of the portal tracts, with progressive fibrosis and cirrhosis developing subsequently. Sclerosing cholangitis (SC) is a frequent finding in children with LCH, but only few cases of adult patients with SC and LCH have been reported [10, 11]. Imaging features are highly variable, depending on the stage of liver involvement, classified in proliferative, granulomatous, xanthomatous, and fibrous phases [11]. Periportal lesions hyperechoic in ultrasonography and hypodense in CT, assuming fat density, have been described in patients with moderately progressing disease [12, 13, 14]. In the patient reported by Radin [13], hyperintense as well as hypointense lesions were seen in T1-weighted MR images, partly showing a mass effect without vessel displacement. In the fibrous phase, multiple nodular hypointense, poorly enhancing periportal areas with spotty calcifications have been described [15]. The features of parenchymal infiltration in our patient differ slightly from these reports, probably due to the more aggressive course of LCH seen in this case. Calcification and T1-weighted hyperintense areas were not present. The peripheral wedge-shaped lesion type with increased enhancement on arterial phase images corresponds well to the findings in primary sclerosing cholangitis (PSC) and may be attributed to decreased portal flow in this area [16, 17]. The disseminated, partly circumscribed hyperechoic and hypoattenuated areas as well as the inhomogeneity emphasized with fat saturation in T1-weighted MR images are compatible with increased fat content. This is presumably related to the foamy consistency of histiocytes in the xanthomatous phase and marked focal steatosis as seen histologically in our case. Lesion-to-liver contrast in the routine T1-weighted fast low-angle shot (FLASH) images was quite poor; hence, the use of fat-saturated or phase-optimized sequences is recommended in these patients. Nevertheless, lesion appearance is largely unspecific in the slice section images, and MRCP is the key to differential diagnosis in this case.

We performed breath-hold MRCP on a 1.5-T system, using the RARE and HASTE technique with spectral fat saturation as described elsewhere [5, 18, 19]. The RARE projection cholangiograms can be obtained in 4 s, allowing breath-hold imaging even in severely ill patients. Magnetic resonance cholangiopancreatography of a normal, non-dilated biliary system depicts the extrahepatic bile ducts and the intrahepatic segmentary ducts up to the first-order branches. Usually peripheral ducts are visualized only in case of dilatation [20, 21]. The pattern of focal cholestasis seen in this case is typical for SC as described in transhepatic cholangiography. Normal appearance of the extrahepatic bile ducts and rarefaction of segmental branches resemble a “pruned tree.” Irregular definition of the remaining ducts with strictures next to normal ducts causes a beading appearance. Particularly the finding of multiple slightly dilated peripheral bile ducts due to ductal obstruction in

several hepatic segments is characteristic of SC [17, 22, 23] and corresponds well with the histologically described pattern of periportal fibrosis with both destruction and proliferation of smaller bile ducts. The short signal void in the CBD seen in MRCP but not in ERCP was presumably artificial in the vicinity of the dilated hepatic artery. This phenomenon is caused by pulsation and compression through the artery and should not be misinterpreted as severe focal stenosis; however, CBD involvement has been reported for either PSC [17] and SC associated with LCH [11].

Diabetes insipidus, cystic destruction of the lung parenchyma, skin lesions, and hepatic involvement resemble a pattern typically seen in LCH, but progressing multiorgan involvement with fatal outcome is a rare finding in an elderly adult. Immunohistochemical proof of S-100 protein expression and particularly ultrastructural evidence of Birbeck granula are characteristic of LCH [1, 4] and inevitable to establish the definitive diagnosis; however, specific imaging can aid in the differential diagnosis before biopsies are sampled. In this case, characteristic imaging findings supported the diagnosis of LCH, but radiologists have to be aware of this rare differential diagnosis in adults. The MRCP appearance was typical for sclerosing cholangitis in an early stage, in which peripheral biliary changes could easily be missed with ERCP. Together with the HRCT revealing characteristic signs of cystic destruction of the lung parenchyma, MRCP served as an important imaging tool in the diagnosis of Langerhans' cell histiocytosis.

References

1. Kilpatrick SE, Wenger DE, Gilchrist GS, Shives TC, Wollan PC (1995) Langerhans' cell histiocytosis (histiocytosis X) of bone. Cancer 76: 2471–2484
2. Favara BE (1991) Langerhans' cell histiocytosis pathobiology and pathogenesis. Semin Oncol 18: 3–7
3. Willman CL, Busque L, Griffith BB, Favara BE, McClain KL, Duncan MH, Gilliland DG (1994) Langerhans'-cell histiocytosis (histiocytosis X): a clonal proliferative disease. N Engl J Med 331: 154–160
4. Siegelman SS (1997) Taking the X out of histiocytosis X. Radiology 204: 322–324
5. Laubenberger J, Büchert M, Schneider B, Blum U, Hennig J, Langer M (1995) Breath-hold projection magnetic resonance-cholangio-pancreaticography (MRCP): a new method for the examination of the bile and pancreatic ducts. Magn Reson Med 33: 18–23
6. Geusens E, Brys P, Ghekiere J, Samson I, Sciot R, Brock P, Baert AL (1998) Langerhans cell histiocytosis of the cervical spine: case report of an unusual location. Eur Radiol 8: 1142–1144
7. Verbist B, Geusens E, Brys P, Verslegers I, Samson I, Sciot R, Baert AL (1998) Langerhans cell histiocytosis of the clavicle: a case report. Eur Radiol 8: 1357–1358
8. Brauner MW, Grenier P, Mouelhi MM, Mompoint D, Lenoir S (1989) Pulmonary histiocytosis X: evaluation with high-resolution CT. Radiology 172: 255–258
9. Moore ADA, Goldwin JD, Müller NL, Naidich DP, Hammar SP, Buschman DL, Takasugi JE, de Carvalho CRR (1989) Pulmonary histiocytosis X: comparison of radiographic and CT findings. Radiology 172: 249–254
10. Scully RE, Mark EJ, McNeely WF, McNeely BU (1993) Case records of the Massachusetts General Hospital. Weekly clinicopathological exercises. N Engl J Med 329: 1108–1115
11. Thompson HH, Pitt HA, Lewin KJ, Longmire WP (1984) Sclerosing cholangitis and histiocytosis X. Gut 25: 526–530
12. Päivänsalo M, Mäkäräinen H (1986) Liver lesions in histiocytosis X: findings on sonography and computed tomography. Br J Radiol 59: 1123–1125
13. Radin DR (1992) Langerhans cell histiocytosis of the liver: imaging findings. Am J Roentgenol 159: 63–64
14. Mampaey S, Warson F, van Hedent E, de Schepper AM (1999) Imaging findings in Langerhans' cell histiocytosis of the liver and the spleen in an adult. Eur Radiol 9: 96–98
15. Arakawa A, Matsukawa T, Yamashita Y, Yoshimatsu S, Ohtsuka N, Miyazaki T, Yamamoto H, Harada M, Ishimaru Y, Takahashi M (1994) Periportal fibrosis in Langerhans' cell histiocytosis mimicking multiple liver tumors: US, CT, and MR findings. J Comput Assist Tomogr 18: 157–159
16. Revelon G, Rashid A, Kawamoto S, Bluemke DA (1999) Primary sclerosing cholangitis: MR imaging findings with pathologic correlation. Am J Roentgenol 173: 1037–1042
17. Ito K, Mitchell DG, Outwater EK, Blasbalg R (1999) Primary sclerosing cholangitis: MR imaging features. Am J Roentgenol 172: 1527–1533
18. Miyazaki T, Yamashita Y, Tsuchigame T, Yamamoto H, Urata J, Takahashi M (1996) MR cholangiopancreatography using HASTE (half-fourier acquisition single-shot turbo spin echo) sequences. Am J Roentgenol 166: 1297–1303
19. Reuther G, Kiefer B, Tuchmann A (1996) Cholangiography before biliary surgery: single-shot MR cholangiography versus intravenous cholangiography. Radiology 198: 561–566
20. Becker CD, Grossholz M, Mentha G, de Peyer R, Terrier F (1997) MR cholangiopancreatography: technique, potential indications, and diagnostic features of benign, postoperative, and malignant conditions. Eur Radiol 7: 865–874
21. Pavone P, Laghi A, Panebianco V, Catalano C, Lobina L, Passariello R (1998) MR cholangiography: techniques and clinical applications. Eur Radiol 8: 901–910
22. Ernst O, Asselah T, Sergent G, Calvo M, Talbodec N, Paris JC, L'Hermine C (1998) MR cholangiography in primary sclerosing cholangitis. Am J Roentgenol 171: 1027–1030
23. Oberholzer K, Lohse AW, Mildenberger P, Grebe P, Schadeck T, Bantelmann M, Thelen M (1998) Diagnosis of primary sclerosing cholangitis: prospective comparison of MR cholangiography with endoscopic retrograde cholangiography. Fortschr Rontgenstr 169: 622–626